Nonlinear surface optical waves in photorefractive crystals with a diffusion mechanism of nonlinearity

G. S. Garcia Quirino, J. J. Sanchez-Mondragon, and S. Stepanov
INAOE, Apartado Postal 51-216, 72000 Puebla, Mexico
(Received 3 March 1994; revised manuscript received 19 August 1994)

A nonlinear optical phenomenon, namely, the surface waves in photorefractive crystals with a diffusion nonlinearity (of the gradient type), is suggested and analyzed. These waves can be guided along the boundary of the crystal with a metal, a dielectric with a lower average refractive index, or a similar photorefractive crystal with the opposite sign of the diffusion nonlinearity. Our estimates predict that for a typical photorefractive crystal such as $BaTiO_3$ this mechanism can ensure efficient concentration of light power in a crystal layer of $\sim 10\ \mu$m thickness.

PACS number(s): 42.65.Jx, 42.65.Hw

I. INTRODUCTION

First experiments on spatial soliton propagation in photorefractive crystals (PRCs) were reported recently in [1,2]. It was demonstrated in these papers (see also the theoretical papers [3,4]) that stable propagation of spatial solitons needs a "quasilocal" drift mechanism of photorefractive nonlinearity similar to that observed in Kerr nonlinear optical media. As it was also shown in [3], the diffusion (gradient-type) mechanism of nonlinearity cannot support stable propagation of the spatial solitons in unlimited PRCs.

On the other hand, some serious efforts were also spent recently for investigation of photorefractive properties of planar waveguide layers formed on the surface of different electro-optic crystals (see, e.g., the review paper [5]). The main practical goal of recent investigations in this area is to increase the light power density in different configurations of photorefractive phase conjugate mirrors based on $BaTiO_3$ and thus to increase the speed of their operation [6].

We suggest and analyze nonlinear surface waves in PRCs with dominant diffusion mechanism of nonlinearity. These guided, spatially confined waves can propagate along the boundary of the crystal with a metallic or a dielectric layer of a lower refractive index or with a similar PRC with the opposite sign of the nonlinearity. In other words, we consider self-channeling of the laser wave along the surface of the PRC without any initially prefabricated waveguide layer.

II. NONLINEAR WAVE EQUATION AND ITS SOLUTION

The basic equation we use below in our analysis is a standard scalar two-dimensional wave equation for the monochromatic light wave [with the frequency ω and complex amplitude $E(x,z)$] propagating in an unlimited, optically transparent medium with some spatial variations of the dielectric constant $\epsilon(x,z)$:

$$[(d^2/dx^2+d^2/dz^2)+\omega^2\epsilon_0\mu_0\epsilon(x,z)]E(x,z)=0\ . \quad (1)$$

This equation is widely used in analysis of the light diffraction from the volume gratings (see, e.g., [7]) and, in particular, in photorefractive crystals (see, e.g., [8]). Unlike this standard problem, however, the dielectric constant $\epsilon(x,z)$ is not fixed here. In our consideration it depends on a spatial light intensity distribution in the propagating wave and is also to be found in a self-consistent way.

Below we shall look for the waves propagating along the z axis which have some fixed profile along the x axis. The complex amplitude of such waves can be written as

$$E(x,z)=E(x)\exp(-i\beta z)\ , \quad (2)$$

where β is the propagation constant of the wave. Since the steady-state nonlinear refractive index changes in PRCs depend on the light intensity but not on its phase, the photoinduced dielectric constant changes also depend on the x coordinate:

$$\epsilon(x,z)=\epsilon+\delta\epsilon(x)\ . \quad (3)$$

Here and below the average (spatially uniform) initial dielectric constant ϵ is supposed to be much higher than its photoinduced change [$\epsilon \gg |\delta\epsilon(x)|$].

Below we limit our consideration to the light waves with real $E(x)$ amplitudes, i.e., to those with plane perpendicular to z-axis wave fronts. This approach is usual for considerations of spatial soliton waves, but by using it we can lose some possible solutions—in particular, in our case, conventional plane waves $E_0\exp(-i\mathbf{K}\cdot\mathbf{r})$ with the $\mathbf{K}$ vector not parallel to the z axis. Indeed, these waves have a uniform distribution of the light intensity and, as a result, they propagate through the photorefractive crystal with diffusion nonlinearity as through an optically linear medium. The stability of such waves as well as the possibility of propagation in PRCs of essentially nonlinear solitonlike waves with non-plane wave fronts need, however, additional more detailed analysis.

Substituting Eqs. (2) and (3) into Eq. (1) results in the following equation for $E(x)$:

$$[d^2/dx^2+(K_0^2-\beta^2)+K_0^2\delta\epsilon(x)/\epsilon]E(x)=0\ , \tag{4}$$

where $K_0=\omega\sqrt{\epsilon\epsilon_0\mu_0}$ is the wave number of the light in an optically linear medium with average refractive index $\sqrt{\epsilon}$. To solve this equation it is necessary to specify the value $\delta\epsilon(x)$, which means introducing some material equation which determines the dependence of $\delta\epsilon(x)$ on $E(x)$. For PRCs with the diffusion mechanism of nonlinearity this can be done rather easily (see, e.g., [8]). Under the steady-state conditions of illumination (when nothing is changing with time) the space-charge electric field arising as a result of drift-diffusion equilibrium equals

$$E_{sc}(x)=-(k_BT/e)[dI(x)/dx]/I(x)\ , \tag{5}$$

where $I(x)$ is the light intensity. Here we assumed a purely electronic type of photoconductivity and neglected possible thermal ionization (i.e., dark conductivity) and saturation of the impurity photorefractive centers in crystal [8].

Taking into account that $[dI(x)/dx]/I(x)=[2dE(x)/dx]/E(x)$ for a purely real function $E(x)$ and that transformation of the space-charge electric field relief to the refractive index changes is ensured via a linear electro-optic effect [8], we obtain

$$\delta\epsilon(x)=2n^4r(k_BT/e)[dE(x)/dx]/E(x)\ . \tag{6}$$

Here r is the linear electro-optic coefficient corresponding to this particular orientation of the PRC and the polarization of the light. For simplicity, here the PRC is assumed to be optically isotropic, which gives $\epsilon=n^2$, where n is the average refractive index of the sample.

Substituting Eq. (6) into Eq. (4) gives the following final differential equation, which in fact proves to be linear:

$$[(d^2/dx^2)/K_0^2+(2\gamma d/dx)/K_0-2\Delta K/K_0]E(x)=0\ . \tag{7}$$

Here $\Delta K=(\beta-K_0)$ is supposed to be much lower than K_0 and $\gamma=K_0n^2r(k_BT/e)$ is the numerical constant characterizing the strength of the diffusion photorefractive nonlinearity, which can vary remarkably in different PRCs. For a typical visible wavelength $\lambda\simeq0.5\ \mu$m, γ is $\sim3\times10^{-3}$ in $BaTiO_3$ and $Sr_xBa_{1-x}Nb_2O_6$ (SBN) and $\sim10^{-5}$ in $Bi_{12}SiO_{20}$, $Bi_{12}TiO_{20}$, and GaAs (see, e.g., [8]). Note that the parameter γ introduced above relates to a widely used photorefractive two-wave mixing gain factor Γ ($=2\pi n^3rE_D/\lambda$ where the diffusion field $E_D=Kk_BT/e$, K is the spatial frequency, and $\Lambda=2\pi/K$ is the fringe spacing of the grating [8]) in a simple way $\Gamma=K\gamma$.

Note here that the final linear equation (7) was obtained from the initial nonlinear one, Eq. (1), where $\epsilon(x)$ depended on the light intensity. It is clearly a direct result of some special "gradient" diffusion photorefractive nonlinearity [Eqs. (5) and (6)]. Since Eq. (7) is of the second order, it is satisfied in particular by two exponential solutions and every linear combination of them also satisfies the same equation. Physically this means that different nonlinear waves with the same ω and β can propagate simultaneously through the crystal without an interaction. It is not true, however, for the waves with different propagation constants β.

Looking for exponential solutions $E(x)\propto\exp(K_0kx)$ of Eq. (7) we obtain

$$k_{1,2}=-\gamma(1\mp\sqrt{1+2\Delta K/K_0\gamma^2})\ . \tag{8}$$

Below we analyze the solutions presented by Eq. (8) in two limit approximations: $2|\Delta K|/K_0\gamma^2\gg1$ (the approximation of a large deviation of the propagation constant β from K_0) and $2|\Delta K|/K_0\gamma^2\ll1$ (the small deviation ΔK approximation).

Large negative values of ΔK in Eq. (8) result in the two solutions with complex, phase conjugate amplitudes from which it is possible to construct two purely real oscillating solutions

$$\begin{aligned}E_1(x)&=\exp(-\gamma K_0x)\cos(x\sqrt{2|\Delta K|K_0})\ ,\\ E_2(x)&=\exp(-\gamma K_0x)\sin(x\sqrt{2|\Delta K|K_0})\ .\end{aligned} \tag{9}$$

If for simplicity (without any restrictions of generality) we assume positive γ in the following consideration, these solutions will decay in the positive direction of the x axis with the exponential factor γK_0 [Fig. 1(a)]. It is clear that these solutions are nothing but simple interference patterns (with the fringe spacing $\Lambda=\lambda/n\sqrt{2|\Delta K|/K_0}$) of two plane waves propagating at the angles $\theta=\mp\arcsin\sqrt{|\Delta K|/2K_0}\simeq\mp\sqrt{|\Delta K|/2K_0}$ counted from the z axis. The amplitudes of these waves, however, are not constant. Because of a unidirectional energy exchange due to two-wave mixing at the photorefractive diffusion hologram recorded in the crystal [i.e., the periodic $\delta\epsilon(x)$ distribution] both of their amplitudes decay exponentially along the x axis.

Note an important difference between the process under consideration and a standard two-wave mixing at a transmittance grating, which is usually analyzed in the photorefractive literature [8]. In the latter case the light wave amplitudes are constant along the x axis (i.e., perpendicular to the grating fringes) and are changing along the z axis. Here we have another configuration of the two-wave mixing process. For the same orientation of the grating fringes (parallel to the z axis) the interacting wave amplitudes are supposed to be constant along the z axis and are changing along the x axis. This means, in fact, that we have two-wave mixing at the reflectance dynamic hologram where intensities of the waves are changing along the direction perpendicular to the grating fringes (i.e., along the x axis in our coordinate system).

On the other hand, large positive ΔK results in solutions similar to standard evanescent waves in optically linear media. There is however, additional decay (for positive γ) of these waves along the x axis with the same exponential factor γK_0 ($k_{1,2}=-\gamma\mp\sqrt{2|\Delta K|/K_0}$) [Fig. 1(b)]. This additional decay clearly results from some uniform change of the refractive index [$\delta\epsilon(x)=\text{const}(x)$ in this case, as follows from Eq. (6)] induced by these two exponentially decaying waves. Note that these two waves decaying in opposite directions produce the refractive index change of the opposite sign.

For the case of low ΔK (i.e., when $2|\Delta K|/K_0\gamma^2\ll1$), the solutions are, however, quite different from those for

the linear medium:

$$E_1(x)=\exp(k_1K_0x)=\exp(-2\gamma K_0x)\ ,$$
$$E_2(x)=\exp(k_2K_0x)=\exp(\Delta Kx/\gamma)\ . \tag{10}$$

For the positive sign of γ, the first ("shallow") wave will decay along the positive direction of the x axis [Figs. 1(c) and 1(d)] with an exponential factor $2K_0\gamma$. Unlike the conventional evanescent waves (which are observed for positive ΔK only), this exponentially decaying wave exists for both positive and negative ΔK and its decrement does not depend on the ΔK value.

In its turn, the second wave E_2 is growing along the x axis for positive ΔK and decaying for negative ΔK. Since $|k_1| \gg |k_2|$, the exponentially decaying wave of this type (or the "deep" wave) can penetrate into the crystal much deeper than the "shallow" wave.

Note here that all these types of nonlinear waves (oscillating and relaxation) are possible in any PRC with this particular γ without any changes in the experimental conditions. Our above separation of two limit cases means that for oscillating (with negative ΔK) solutions presented by Eq. (9), $|\Delta K|$ proves to be rather high ($\geq K_0\gamma/2$). On the other hand, for the relaxation-type solutions decaying in the same direction for negative ΔK [Eq. (10)], $|\Delta K|$ proves to be low ($\leq K_0\gamma/2$). For the boundary value $|\Delta K| \simeq K_0\gamma/2$, the transfer of the oscillation type of the solutions into the relaxation one is observed.

III. LOCALIZED SURFACE WAVE SOLUTIONS

Below we are interested in the consideration of the guided waves which can propagate along the boundary of the photorefractive medium (which in the following analysis is supposed to occupy the semiplane with positive $x>0$) and can be constructed using the solutions obtained above. For this purpose only the solutions for negative ΔK are suitable. Indeed both functions presented in Figs. 1(a) and 1(c) decay in the positive direction of the x axis. As a result, by taking some linear combinations of two functions obtained for the same value of negative ΔK one can satisfy necessary boundary conditions and obtain the guided solution decaying with $x \Longrightarrow \mp\infty$.

We will discuss three basic cases: (i) the boundary PRC–ideal metal, (ii) the boundary PRC–optically linear transparent dielectric with lower refractive index $n_1=n-\delta n$, and (iii) the boundary PRC–PRC′ (with the

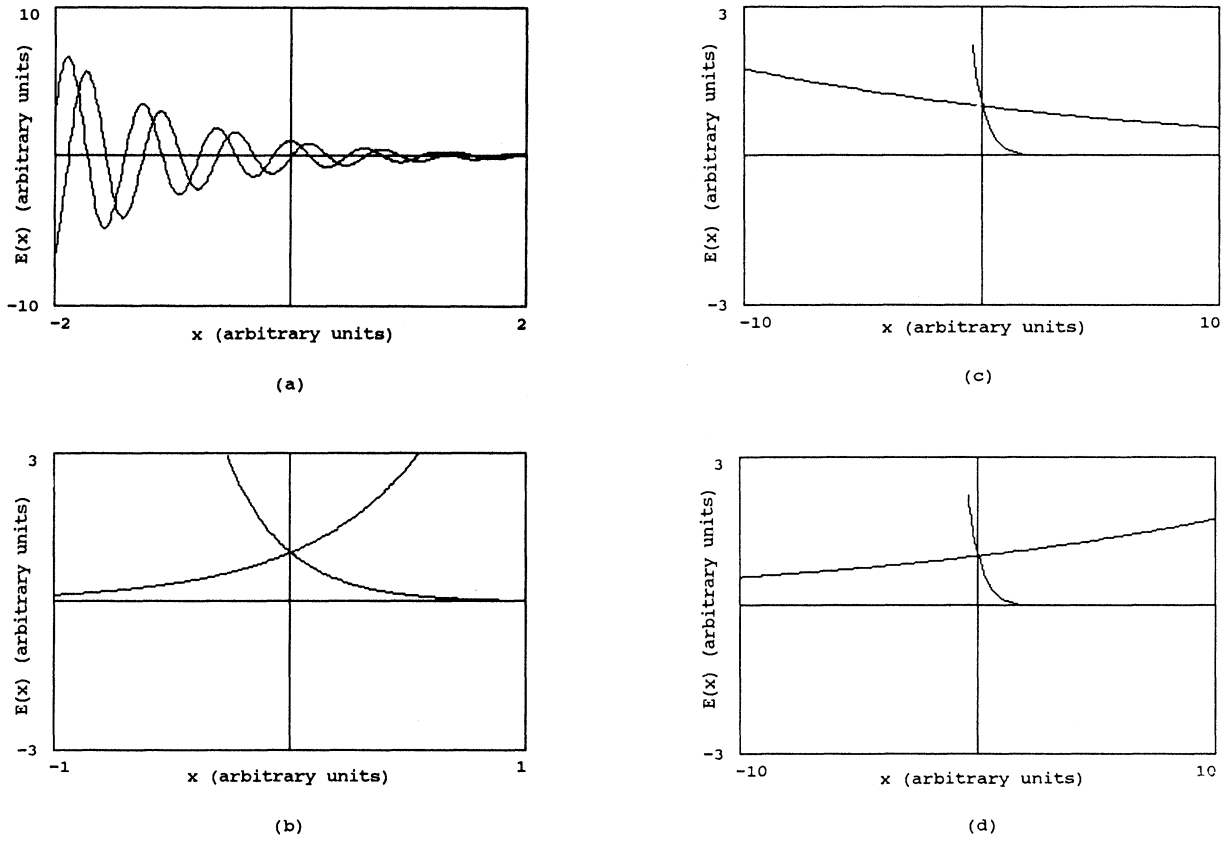

FIG. 1. Complex amplitude $E(x)$ in typical nonlinear waves for the photorefractive crystal with diffusion (gradient-type) nonlinearity: (a) oscillating sinusoidal and cosinusoidal solutions for large negative ΔK (curves correspond to $\gamma K_0=1$ and $K=\sqrt{2|\Delta K|K_0}=10$); (b) evanescent waves for large positive ΔK (curves correspond to $\gamma K_0=1$ and $\sqrt{2|\Delta K|K_0}=3$; (c) exponential solutions for small negative ΔK (curves correspond to $\gamma K_0=1$ and $|\Delta K|/\gamma=\frac{1}{18}$; (d) exponential solutions for small positive ΔK (curves correspond to $\gamma K_0=1$ and $|\Delta K|/\gamma=\frac{1}{18}$).

same n, but with negative γ). Here we limit our consideration to only these three cases, having in mind that there can be more complicated situations which need more detailed analyses. Even in this case we simplify the analysis by assuming that the boundary between two different media does not possess any particular properties (e.g., surface trapping centers, blocking properties for the charge transfer, surface photogalvanic effects, etc.).

Propagation along the idealized metal surface (i.e., the case when the tangent components of the electric field equal zero at the boundary of PRC) is the most simple. The first type of the guided wave (for the large negative ΔK), the oscillating guided wave, is represented here by the second, sinusoidal oscillating solution [Eq. (9)]; see Fig. 2(a). The second type of guided wave can be constructed as a linear combination of the shallow and deep exponential waves with small negative ΔK [Eq. (10)]:

$$E(x)=\exp(\Delta K x/\gamma)-\exp(-2\gamma K_0 x)\ ; \tag{11}$$

see Fig. 2(b).

One can see that the first (oscillating) guided wave is characterized by the fixed penetration depth $d_0 \sim 1/\gamma$, independent of the interference fringe spacing K inside the PRC. On the other hand, the other (relaxation-type) guided wave can have a much larger penetration depth $d_0=\gamma/|\Delta K|$, increasing inversely proportionally to $|\Delta K|$.

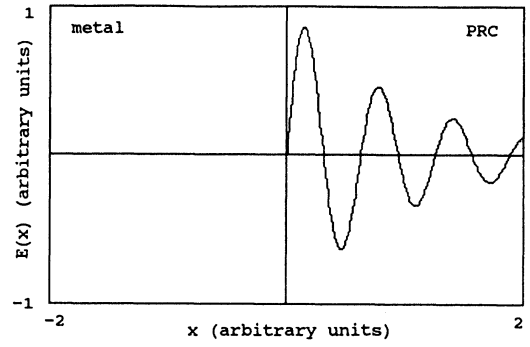

(a)

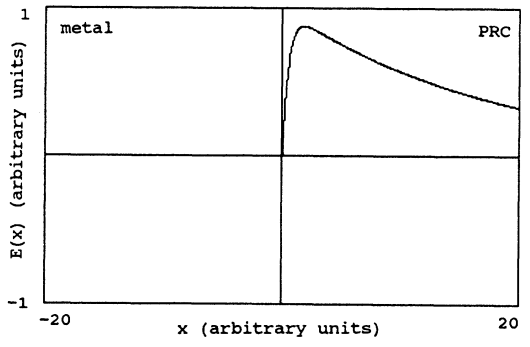

(b)

FIG. 2. Complex amplitude $E(x)$ in surface nonlinear waves near the plane boundary PRC–ideal metal: (a) for large negative ΔK (curve corresponds to $\gamma K_0=1$ and $K=\sqrt{2|\Delta K|K_0}=10$) and (b) for small negative ΔK (curve corresponds to $\gamma K_0=1$ and $d_0^{-1}=|\Delta K|/\gamma=\frac{1}{18}$).

For the case of a boundary with the linear dielectric medium with a lower average refractive index ($\delta n>0$), the guided waves can be easily constructed for the case of large negative ΔK. Here the solutions of Eq. (9) correspond to the standing wave along the x axis (with additional comparatively slow decay). So the behavior of the guided wave near the boundary [Figs. 3(a)–3(c)] reminds one of a conventional planar dielectric waveguide with approximately the same refractive index difference δn between the core and the cladding [9].

The penetration depth into the dielectric medium can be expressed through δn and the spatial frequency of the grating in the PRC (K) is given by

$$d_1=(2K_0^2\delta n/n-K^2)^{-1/2}\ . \tag{12}$$

This means in particular that the higher the spatial frequency K of the interference pattern in the PRC, the higher the refractive index change δn one needs to ensure propagation of the surface guided wave ($\delta n^{\min}=nK^2/2K_0^2$).

In the same way, the relaxation type of guided waves [Fig. 3(d)] can be constructed for this boundary from the solutions for small ΔK [Eq. (10)]. In this case

$$d_1=(2K_0^2\delta n/n-2K_0\gamma/d_0)^{-1/2} \tag{13}$$

and the minimal δn value necessary for wave guiding equals $\delta n^{\min}=n\gamma/K_0 d_0$. As in the previous case, if the condition $\delta n>\delta n^{\min}$ is satisfied, the larger the δn, the lower the observed penetration depth in the dielectric [Figs. 3(a)–3(c)].

For the boundary between two PRCs with the opposite sign of γ, both symmetric and antisymmetric types of guided waves are clearly possible. Their structure for both large and small negative ΔK is presented in Fig. 4. Note that the antisymmetric solution in the volume of every PRC corresponds to that for the boundary with the ideal metal surface (Fig. 2), which clearly results from the imaging property of an ideal metal surface. Nonsymmetric guided waves, which are linear combinations of symmetric and antisymmetric solutions, can also be observed for the boundary of two PRCs.

IV. DISCUSSION

Let us estimate the possible penetration depths into typical PRCs of the guided waves under consideration. For oscillating guided waves d_0 is fixed and equals $(\gamma K_0)^{-1}$, which, in accordance with the γ values given above, results in $d_0 \simeq 10$ μm for $BaTiO_3$ and $\simeq 2$ mm for cubic PRCs of the $Bi_{12}SiO_{20}$ family. Even larger penetration depths are expected for GaAs since we use longer wavelengths here.

This means that the most promising PRC for experimental observation of the nonlinear surface waves is ferroelectric photorefractive $BaTiO_3$ or SBN. Here the efficient concentration of the propagating waves in the surface layer with the thickness comparable to that [6]

typical for the prefabricated planar waveguides can be observed for the simple diffusion mechanism of nonlinearity. So this self-channeling of the light waves near the PRC surface can probably be used for efficient concentration of the light beam power in different phase conjugate configurations in these ferroelectric PRCs.

There is also an efficient way to increase γ (and, as a result, to reduce the penetration depth of the guided waves) in cubic PRCs, namely, to apply the ac electric field. It is known [8] that in this case it is possible to record efficient shifted phase holograms corresponding to the gradient type of photorefractive nonlinearity. Instead of $k_B T/e$ one can formally substitute $\mu\tau E_{ac}^2$ in Eq. (5) (here μ and τ are the mobility and the lifetime of the carriers, respectively, and E_{ac} is the amplitude of the applied square-wave electric field). For $E_{ac} \simeq 10$ kV/cm and $\mu\tau \simeq 10^{-7}$ cm^2/V, typical for $Bi_{12}SiO_{20}$ and $Bi_{12}TiO_{20}$ crystals [8], this also gives $\gamma \sim 3 \times 10^{-3}$, i.e., the value of γ obtained above for highly efficient $BaTiO_3$.

This case needs, however, a more detailed analysis since the nonlocal (gradient-type) photorefractive nonlinearity under the external ac field was investigated earlier mainly for sinusoidal interference patterns with low contrast. The real penetration depth of the surface wave in $Bi_{12}SiO_{20}$-type crystals will probably be somewhere between these two estimates (2 mm and 10 μm) obtained above.

Note that the crystal cut for observation of the nonlinear photorefractive surface waves sometimes is the same and is sometimes not the same as that for the standard holographic experiment; this is true in particular for $BaTiO_3$ [8]. Without discussing the details (optimal crystallographic orientation and the light polarization can differ in different PRCs), note that efficient propagation of the surface waves is possible along the sample boundaries parallel to the layers of the holographic grating, which is efficiently reconstructed in this PRC for this particular light polarization.

Another very important characteristic feature of the nonlinear photorefractive waves under consideration is their independence of the light intensity. It is a direct result of a very special optical nonlinearity mechanism for which the photoinduced refractive index changes do not depend on the light intensity [Eq. (3)]. This means that, as in the experiments with photorefractive spatial solitons [1,2], very low (μW) levels of cw laser power can be used here.

Note that rather fast decay of the surface wave intensi-

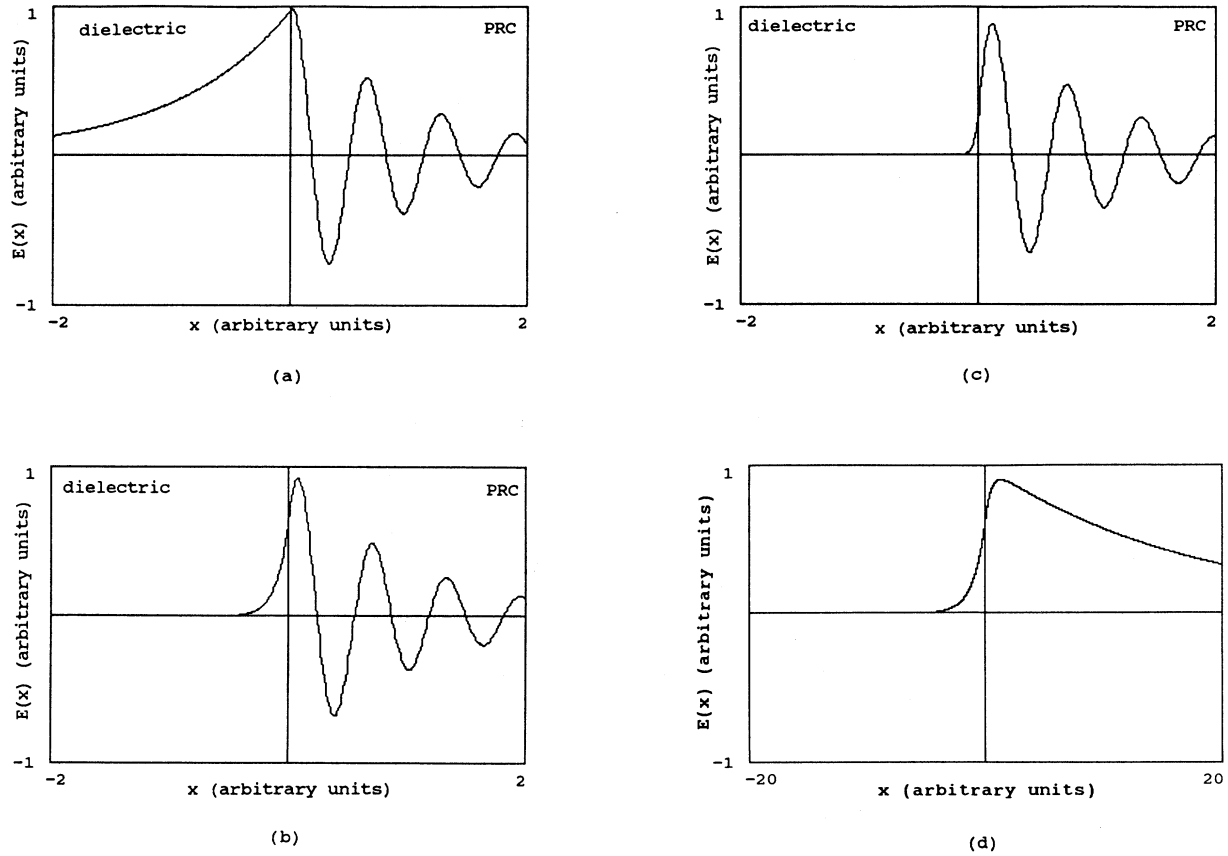

FIG. 3. Complex amplitude $E(x)$ in surface nonlinear waves (of TE type) near the plane boundary PRC–dielectric with lower average refractive index: (a)–(c) oscillating solutions for large negative ΔK [curves correspond to $\gamma K_0 = 1$, $K = \sqrt{2|\Delta K|K_0} = 10$, and $d_1^{-1} = 1$, 10, and 30 for (a), (b), and (c), respectively]; (d) exponential solution for small negative ΔK (curve corresponds to $\gamma K_0 = 1$, $d_0^{-1} = |\Delta K|/\gamma = \frac{1}{18}$, and $d_1^{-1} = 1$).

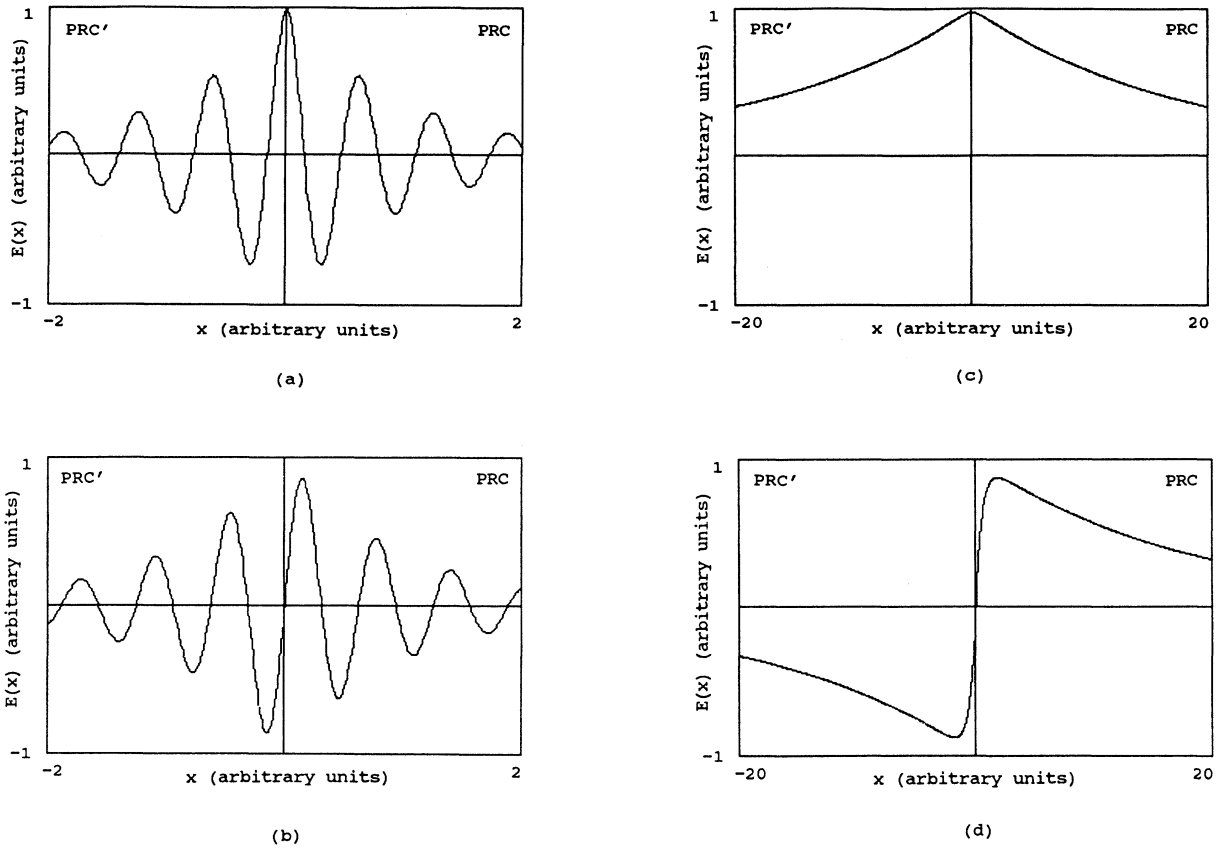

FIG. 4. Complex amplitude $E(x)$ in surface nonlinear waves (of TE type) near the plane boundary PRC-PRC' with the opposite sign of nonlinearity: (a) and (b) symmetric and antisymmetric solutions for large negative ΔK (curves correspond to $\gamma K_0 = 1$ and $K = \sqrt{2|\Delta K|K_0} = 10$); (c) and (d) symmetric and antisymmetric waves for small negative ΔK (curves correspond to $\gamma K_0 = 1$ and $d_0^{-1} = |\Delta K|/\gamma = \frac{1}{18}$.

ty along the x axis means that the above analysis is applicable basically to rather thin (in the x direction) samples of PRCs. Indeed, for a bulk sample the photoconductivity induced by the light wave will sooner or later be comparable to the dark conductivity of the sample. This means that the original approximation of the negligibly low thermal ionization rate in Eq. (5) is not valid for this region. Clearly this complication needs additional, more detailed analysis, but qualitatively the main effect is the following (see also [10]). The dark conductivity reduces the efficiency of the photorefractive two-wave interaction (i.e., the efficient value of γ). As a result, the steep decay of the surface wave near the boundary will be replaced by a flatter one in the depth of the sample, where the photoconductivity is comparable to the dark conductivity.

The detailed analysis of the exponentially decaying ("evanescent") nonlinear waves in the PRCs presented above is closely related to another interesting problem, namely, to bistability in the reflection from the boundary of dielectric and photorefractive media. This problem was analyzed originally for conventional Kerr optical nonlinearity in [11]. Recently bistability in the reflection properties of a boundary between linear and photorefractive media was considered in [10,12] as well.

V. CONCLUSION

Summarizing, we suggested and analyzed an optical nonlinear effect—the guided surface waves in photorefractive crystals with the diffusion (gradient-type) mechanism of nonlinearity. The analysis predicts that in ferroelectric photorefractive $BaTiO_3$ it is possible to observe efficient waveguiding near the sample surface within the layers of $\sim 10\,\mu$m thickness.

Some other important questions are to be investigated in relation to these nonlinear photorefractive surface waves. Among them are the above-mentioned influence of the crystal dark conductivity, the stability of the self-guided solutions obtained, and the interaction of the nonlinear waves with different propagation constants.

Note added. After this manuscript was submitted for publication, Daisy and Fisher published another, more extended, paper [13] with a theoretical analysis of bistability in the reflection from the interface between linear and photorefractive media.

ACKNOWLEDGMENT

The authors would like to express their sincere gratitude to Dr. N. Korneev for stimulating discussions and useful comments.

[1] G. Duree, J. Shultz, G. J. Salamo, M. Segev, A. Yariv, B. Crosignani, P. Di Porto, E. J. Sharp, and R. R. Neurgaonkar, Phys. Rev. Lett. **71**, 533 (1993).

[2] M. D. Iturbe Castillo, P. A. Marquez Aguilar, J. J. Sanchez Mondragon, S. Stepanov, and V. Vysloukh, Appl. Phys. Lett. **64**, 1 (1994).

[3] M. Segev, B. Crosignani, A. Yariv, and B. Fisher, Phys. Rev. Lett. **68**, 923 (1992).

[4] B. Crosignani, M. Segev, D. Engin, P. Di Porto, A. Yariv, and G. Salamo, J. Opt. Soc. Am. B **10**, 446 (1993).

[5] E. van Wood, P. J. Cressman, R. L. Holman, and C. M. Verber, in *Photorefractive Materials and their Applications,* edited by P. Guenter and J.-P. Huignard (Springer-Verlag, Berlin, 1989), Vol. II.

[6] K. E. Younden, S. W. James, R. W. Eason, P. J. Chandler, L. Zhang, and P. D. Townsend, Opt. Lett. **17**, 1509 (1992).

[7] H. Kogelnik, Bell Syst. Tech. J. **48**, 2909 (1969); R. G. Collier, C. B. Burckhardt, and L. H. Lin, *Optical Holography* (Academic, New York, 1971).

[8] M. P . Petrov, S. I. Stepanov, and A. V. Khomenko, *Photorefractive Crystals in Coherent Optical Systems* (Springer-Verlag, Berlin, 1991).

[9] D. Marcuse, *Light Transmission Optics* (Van Nostrand, New York, 1972).

[10] R. Daisy and B. Fisher (unpublished).

[11] A. E. Kaplan, Pis'ma Zh. Eksp. Teor. Fiz. **24**, 132 (1976) [JETP Lett. **24**, 114 (1976)]; Zh. Eksp. Teor. Fiz. **72**, 1710 (1977) [Sov. Phys. JETP **45**, 896 (1977)]; IEEE J. Quantum Electron. **QE - 17**, 336 (1981).

[12] R. Daisy and B. Fisher, Opt. Lett. **17**, 847 (1992).

[13] R. Daisy and B. Fisher, J. Opt. Soc. Am. B **11**, 1059 (1994).